Antemortem vs Postmortem Histopathologic and Ultrastructural Findings in Paired Transbronchial Biopsy Specimens and Lung Autopsy Samples From Three Patients With Confirmed SARS-CoV-2

Daniel Gagiannis, MD,[1,] Vincent Gottfried Umathum, MD,[2,*] Wilhelm Bloch, MD,[3] Conn Rother, MD,[4] Marcel Stahl, MD,[1] Hanno Maximilian Witte, MD,[2,4,5] Sonja Djudjaj, PhD,[6] Peter Boor, MD, PhD,[6] and Konrad Steinestel, MD, PhD[2,]*

From the [1]Department of Pulmonology, [2]Institute of Pathology and Molecular Pathology, and [4]Department of Hematology and Oncology, Bundeswehrkrankenhaus Ulm, Ulm, Germany; [3]Department of Molecular and Cellular Sport Medicine, German Sport University Cologne, Cologne, Germany; [5]Department of Hematology and Oncology, University Hospital Schleswig-Holstein Campus Luebeck, Luebeck, Germany; and [6]Institute of Pathology, RWTH Aachen University Hospital, Aachen, Germany.

ABSTRACT

Objectives: Respiratory failure is the major cause of death in coronavirus disease 2019 (COVID-19). Autopsy-based reports describe diffuse alveolar damage (DAD), organizing pneumonia, and fibrotic change, but data on early pathologic changes and during progression of the disease are rare.

Methods: We prospectively enrolled three patients with COVID-19 and performed full clinical evaluation, including high-resolution computed tomography. We took transbronchial biopsy (TBB) specimens at different time points and autopsy tissue samples for histopathologic and ultrastructural evaluation after the patients' death.

Results: Severe acute respiratory syndrome coronavirus 2 (SARS-CoV-2) was confirmed by reverse transcription polymerase chain reaction and/or fluorescence in situ hybridization in all TBBs. Lung histology showed reactive pneumocytes and capillary congestion in one patient who died shortly after hospital admission with detectable virus in one of two lung autopsy samples. SARS-CoV-2 was detected in two of two autopsy samples from another patient with a fulminant course and very short latency between biopsy and autopsy, showing widespread organizing DAD. In a third patient with a prolonged course, autopsy samples showed extensive fibrosis without detectable virus.

Conclusions: We report the course of COVID-19 in paired biopsy specimens and autopsies, illustrating vascular, organizing, and fibrotic patterns of COVID-19–induced lung injury. Our results suggest an early spread of SARS-CoV-2 from the upper airways to the lung periphery with diminishing viral load during disease.

KEY POINTS

- There is interindividual, anatomic, and chronological variability in the histologic presentation of coronavirus disease 2019 (COVID-19) in the lung, and data on early changes in living patients are rare.
- COVID-19 spreads from central airways to the periphery, and COVID-19–associated lung injury may present as diffuse alveolar damage (DAD), organizing DAD/acute fibrinous and organizing pneumonia, or fibrosis.
- Severe COVID-19 may result in significant fibrotic change in the lung parenchyma—with no detectable virus at this stage of the disease.

KEY WORDS

COVID-19; SARS-CoV-2; ARDS; Lung pathology; Diffuse alveolar damage; Organizing pneumonia; Lung fibrosis

Am J Clin Pathol XXXX 2021;XX:1–0
HTTPS://DOI.ORG/10.1093/AJCP/AQAB087

Received: February 2, 2021
Accepted: April 20, 2021
Advance publication: August 31, 2021

Corresponding author: Konrad Steinestel, MD, PhD; konradsteinestel@bundeswehr.org.

*First authors.

Funding: This work was supported in part by the German Registry of COVID-19 Autopsies (www.DeRegCOVID.ukaachen.de), funded by the Federal Ministry of Health (ZMVI1-2520COR201), and the Federal Ministry of Education and Research within the framework of the network of university medicine (DEFEAT PANDEMIcs, 01KX2021).

INTRODUCTION

Since severe acute respiratory syndrome coronavirus 2 (SARS-CoV-2) and the resulting disease, coronavirus disease 2019 (COVID-19), emerged in late 2019, much effort has been put in a better understanding of the clinical course of the disease. While most patients have rather mild symptoms, some patients—especially those sharing risk factors such as older age, cardiovascular disease, or chronic obstructive pulmonary disease—are at risk of developing life-threatening respiratory failure.[1] Early autopsy studies conducted in China described diffuse alveolar damage (DAD) with an early edematous phase followed by hyaline membrane formation, desquamation of pneumocytes, and an increased interstitial mononuclear infiltrate.[2] In one case, Tian et al[3] reported loose intra-alveolar fibromyxoid proliferation reminiscent of organizing pneumonia (OP). In the meantime, it is widely accepted that COVID-19 follows a biphasic pattern of an initial viral response phase followed by an inflammatory second phase and that mortality is linked primarily to the development of acute respiratory distress syndrome (ARDS).[1,4] Based on a meta-analysis of 131 reported autopsy cases, Polak et al[5] postulated that the main histologic patterns of COVID-19–related lung injury can be categorized into epithelial (reactive changes and DAD), vascular (microvascular damage, thrombi, and OP) and fibrotic, but these patterns may overlap and be coexistent in the same patient at a given time point. Nicholson et al[6] proposed that an initial (pre)exudative phase of DAD (0-7 days) is followed by an organizing phase (1 week to months) and might ultimately progress to fibrosis (months). A specific subtype of organizing DAD and OP with ball-like fibrin and fibromyxoid plugging, designated acute fibrinous and organizing pneumonia (AFOP), has also been described in COVID-19 autopsy cases.[7] The exact mechanisms of SARS-CoV-2–related ARDS development are not fully understood. It has been postulated that the severity of COVID-19 might correlate with a hyperinflammatory response and uncontrolled secretion of cytokines, showing similarities to cytokine releasing syndrome,[8] but cytokine levels in severe cases of COVID-19 are lower compared with those in patients with severe influenza.[9] Overlapping clinical, serologic, and imaging features between severe COVID-19 and lung manifestation of autoimmune disease, such as systemic lupus erythematosus or systemic sclerosis, have been described, and in one study, the presence of autoantibodies (antinuclear antibodies [ANAs] and extractable nuclear antibodies [ENAs]) was significantly associated with a need for intensive care treatment and the occurrence of severe complications.[10] This finding has now been confirmed by others and might be attributed to extrafollicular B-cell activation with excessive production of antibody-secreting cells in critically ill patients with COVID-19.[11-13] A better understanding of the pathophysiology of lung injury in COVID-19 would also shed light on the urgent question of long-term sequelae of the disease in millions of COVID-19 survivors. Despite a large number of autopsy studies that represent a snapshot of the disease at the time of death, to our knowledge no study has compared *antemortem* vs *postmortem* histopathologic and ultrastructural features of COVID-19. We report here the histopathology of transbronchial biopsy specimens and autopsy samples together with reverse transcription polymerase chain reaction (RT-PCR)– and fluorescence in situ hybridization (FISH)–based detection of SARS-CoV-2 and ultrastructural analyses from three patients with confirmed SARS-CoV-2 infection.

MATERIALS AND METHODS

We consecutively included three patients with positive SARS-CoV-2 RT-PCR (mucosal swab) admitted to our hospital in March and April 2020 after obtaining informed consent. Patients or their relatives had given written informed consent to routine diagnostic procedures (serology, bronchoscopy, radiology) as well as (partial) autopsy in the case of death, respectively, as well as to the scientific use of data and tissue samples in the present study. This project was approved by the local ethics committee (reference No. 129-20) and conducted in accordance with the Declaration of Helsinki.

Clinical Characteristics

We collected clinical information from electronic patient files. Data included disease-related events, preexisting comorbidities, imaging, and clinical follow-up. Baseline clinical characteristics are given in **TABLE 1**. The "Berlin definition" was used to categorize ARDS.[14] The Horovitz quotient (PaO_2/FiO_2) was assessed in all ARDS cases based on arterial blood gas analysis. During intensive care unit (ICU) treatment, ventilation parameters, duration of invasive ventilation, catecholamine support, prone positioning, Murray lung injury score, and the need for additional temporary dialysis were continuously assessed.[15] A profitable trial of prone positioning was defined by an increasing Horovitz

TABLE 1 Clinical Characteristics of Patients With COVID-19

Characteristic	Patient 1	Patient 2	Patient 3
Age, y	80s	60s	50s
Sex	Male	Female	Male
Preexisting diseases			
Cardiovascular risk factors[a]	x	x	—
Cardiovascular disease[b]	x	x	—
Oncologic disease	x	—	—
Rheumatic disease	—	x	—
Smoking history (pack years)	x (40)	—	x (40)
Lactate dehydrogenase, U/L (reference, ≤240)	292	449	414
D-dimer, mg/L (reference, ≤0.5)	>30	3.65	0.92
C-reactive protein, mg/dL (reference, ≤0.5)	42.1	25.2	5.6
IL-6, pg/mL (reference, ≤10)	2,205	646	2,093
ANA/ENA			
ANA titer (reference IIF, <1:100)	1:100	1:1,000	1:100
ENA (reference IB, negative)	—	—	x (Scl-70)

ANA, antinuclear antibody; ENA, extractable nuclear antigen; IB, immunoblot; IIF, indirect immunofluorescence; IL-6, interleukin 6; x, present; —, none/absent.
[a]Diabetes mellitus, dyslipidemia, arterial hypertension, obesity, nicotine abuse.
[b]Coronary disease, post–myocardial infarction, peripheral arterial vaso-occlusive disease, poststroke, atherosclerosis.

HTTPS://DOI.ORG/10.1093/AJCP/AQAB087

quotient of 30 mm Hg or more. One entire trial covered 16 hours of sustained prone positioning.

Serology/Laboratory Values

Laboratory values upon admission to the ICU included D-dimers, lactate dehydrogenase (LDH), interleukin 6 (IL-6), and C-reactive protein (CRP) TABLE 1. ANA/antineutrophil cytoplasmic antibody/ENA screening was performed as previously described.[10]

Imaging

Imaging was performed on a Somatom Force Scanner (Dual Source Scanner 2*192 slices; Siemens) in accordance with the guidelines of the German Radiological Society and our hospital's COVID-19 guidelines, using low-dose computed tomography (CT) with high-pitch technology.[16] The following parameters were used: tube voltage (100 kV with tin filtering) and tube current (96 mAs with tube current modulation). In two cases, examination was performed as a non–contrast-enhanced full-dose protocol because of suspected interstitial lung disease, in one case as a contrast-enhanced CT scan to exclude pulmonary thromboembolism. The x-ray examinations were performed at the respective wards as bedside x-ray examinations (Mobilett Mira Max; Siemens) as a single anterior-posterior view. The CT images were evaluated according to the Expert Consensus Statement of the Radiological Society of North America and classified as typical, indeterminate, atypical, and negative appearance for COVID-19.[16,17]

Histology and SARS-CoV-2 Detection

Lung tissue specimens were obtained from transbronchial biopsies (TBBs). In three deceased patients, partial autopsies were performed in which lung (central and peripheral areas), heart, and liver tissues were sampled extensively. Specimens were stained with H&E, phosphotungstic acid hematoxylin, Elastica-van-Gieson, and Masson-Goldner. For SARS-CoV-2, fluorescence in situ hybridization (FISH) paraformaldehyde-fixed, paraffin-embedded 1-µm sections of TBB specimens and lung autopsy material were deparaffinized followed by dehydration with 100% ethanol. FISH was performed with the RNAscope Multiplex Fluorescent Reagent Kit v2 assay (Advanced Cell Diagnostics) according to the manufacturer's instruction. Briefly, a heat-induced target retrieval step followed by protease was performed. Afterward, sections were incubated with the following RNAscope Probe: V-nCoV2019-S (#848561-C1), V-nCoV2019-S-sense (#845701-C1), Hs-ACE2-C2 (#848151-C2), and Hs-TMPRSS2-C2 (#470341-C2). After the amplifier steps, the fluorophores Opal 570 and 650 (PerkinElmer Life and Analytical Sciences) were applied to the tissues incubated with the C1 and C2 probe, respectively. Finally, nuclei were stained with DAPI, and the slides were mounted with ProLong Gold antifade reagent (Invitrogen). Sections were analyzed with Zeiss Axio Imager 2 and image analysis software (ZEN 3.0 blue edition). SARS-CoV-2 RNA was extracted using the Maxwell 16 FFPE Plus Tissue LEV DNA Purification KIT (Promega) on the Maxwell 16 IVD Instrument (Promega). Using the TaqMan 2019-nCoV kit (ThermoFisher), detection of the SARS-CoV-2 E gene was performed according to the manufacturer's instructions.

Electron Microscopy

Lung tissue was immersion fixed with 4% paraformaldehyde in 0.1 mol/L phosphate-buffered saline (PBS), pH 7.4. After several washing steps in 0.1 mol/L PBS, tissue was osmicated with 1% OsO_4 in 0.1 mol/L cacodylate and dehydrated in increasing ethanol concentrations. Epon infiltration and flat embedding were performed following standard procedures. Methylene blue was used to stain semithin sections of 0.5 µm. Then, 70- to 90-nm-thick sections were cut with an Ultracut UCT ultramicrotome (Reichert) and stained with 1% aqueous uranylic acetate and lead citrate. Samples were studied with a Zeiss EM 109 electron microscope (Zeiss) coupled to a TRS USB (2,048 × 2,048, v.596.0/466.0) camera system with ImageSP ver.1.2.6.11 (x64) software (Sysprog).

RESULTS

Baseline Patient Characteristics and Clinical Course of the Disease

The study included two male patients and one female patient who were hospitalized for RT-PCR–confirmed SARS-CoV-2 infection. The timeline of disease course is depicted in FIGURE 1A. Baseline laboratory values and clinical characteristics are summarized in TABLE 1. Of note, ANA screening by indirect immunofluorescence was positive in all three patients; in patient 2, the titer was 1:1,000, and in patient 3, a specific autoantibody (Scl-70) could be detected by immunoblot. While patients 1 and 3 had to undergo invasive ventilation 2 and 3 days after the diagnosis of COVID-19, patient 2 was transferred from another hospital in a critical state. In patient 1, TBB was performed before knowledge of a positive SARS-CoV-2 test result (day 0). This patient died of pulmonary thromboembolism 5 days later. Except for the continuation of a treatment protocol with hydroxychloroquine and azithromycin that had been established in the previous hospital for patient 2, no specific therapeutic regimens were administered to patients 1 and 3. TBBs in patients 2 and 3 were performed after 13 and 23 days of ICU treatment, respectively, to assess the fibrotic change of lung parenchyma and to evaluate a possible use for antifibrotic treatment options. An autopsy was performed in all three cases on the day after the patients' death following the published guidelines.[18]

Imaging

Representative CT scans from all patients are shown in FIGURE 1B, FIGURE 1C, and FIGURE 1D. While there was a discrete nonspecific interstitial pneumonia-like pattern with only minimal ground-glass opacities (GGOs) in patient 1, patient 2 showed far more widespread GGOs combined with consolidations and a positive aerobronchogram, suggestive of OP. In patient 3, imaging showed severe parenchymal damage with diffuse GGOs, bronchiectasis, cyst formation, and air trapping.

Histopathologic Findings in Vital TBB Specimens and Lung Autopsy Samples

The main finding in TBB specimens from patient 1 was reactive changes of pneumocytes (desquamation, multinucleation) together with a discrete interstitial mononuclear infiltrate. In some alveoli, there was

HTTPS://DOI.ORG/10.1093/AJCP/AQAB087

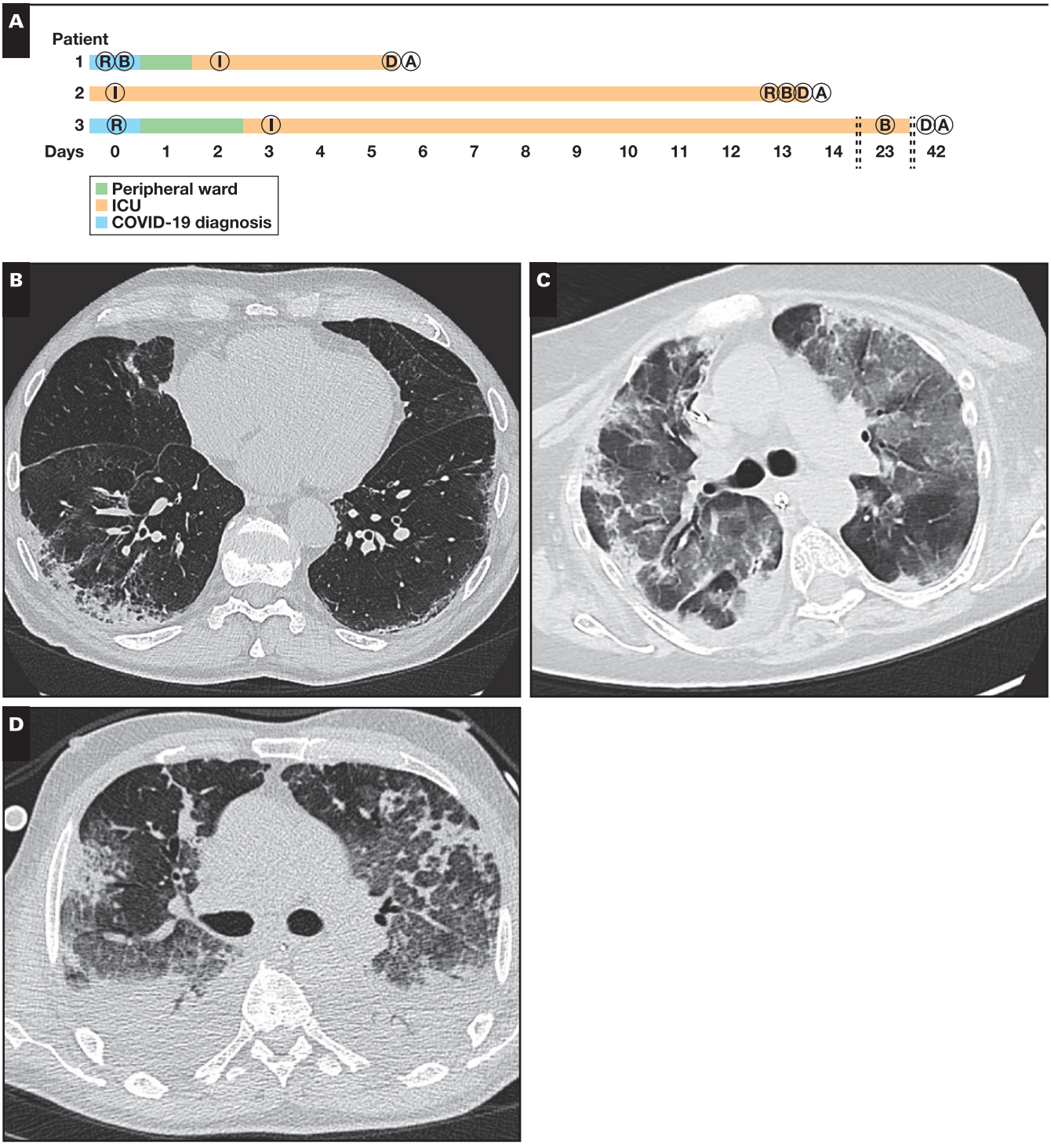

FIGURE 1 **A**, Timeline of the disease course in three patients with coronavirus disease 2019 (COVID-19). While patients 1 and 3 were treated in the peripheral ward after diagnosis, patient 2 was taken over from another hospital while immediate intubation (I) was required. Periods in the intensive care unit (ICU) ranged from 4 to 39 days. Transbronchial biopsy (TBB) specimens were taken on the day of hospital admission (patient 1), day 14 (patient 2), and day 23 (patient 3). Imaging was performed on the day of hospital admission (patients 1 and 3) or before TBB (day 13, patient 2). Autopsies (A) were performed 1 day after death (D) in all three patients. B, biopsy; R, imaging. **B-D**, Results from imaging. Imaging in patient 1 showed a nonspecific interstitial pneumonia-like pattern with minimal ground-glass opacities (GGOs) in the left subpleural space (**B**). In patient 2, there were diffuse GGOs and both subpleural and peribronchial consolidations with a positive aerobronchogram resembling organizing pneumonia (**C**). Imaging in patient 3 showed parenchymal lung injury with diffuse GGOs, bronchiectasis, cysts, and air-trapping (**D**).

HTTPS://DOI.ORG/10.1093/AJCP/AQAB087

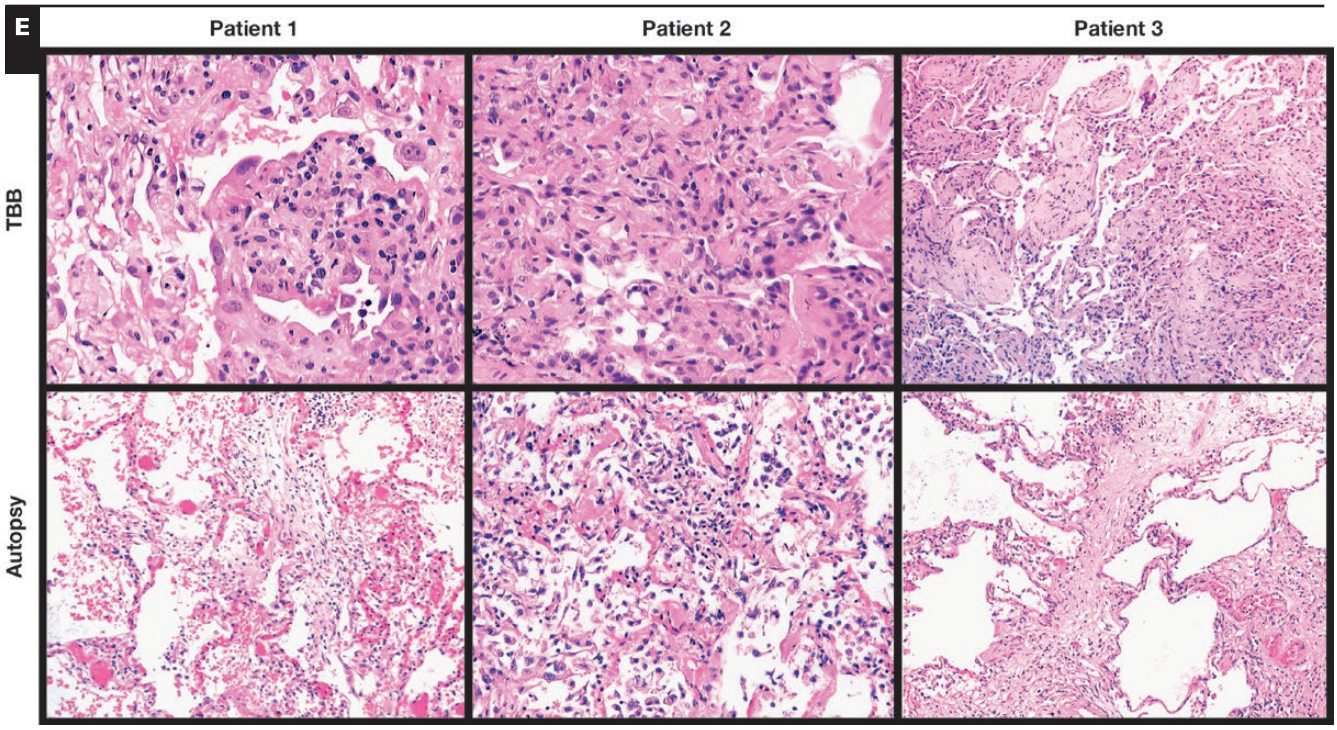

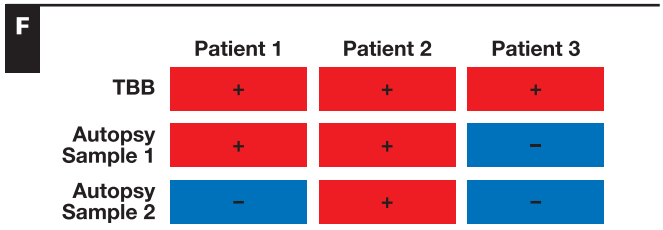

FIGURE 1 (cont) **E**, Representative histology images (H&E). TBB specimens in patient 1 showed reactive pneumocyte changes and loose fibromyxoid plugging with capillary congestion in autopsy samples; in patient 2, TBB specimens showed alveolar collapse with fibrin deposition and plug-like fibromyxoid organization (acute fibrinous and organizing pneumonia–like pattern) in autopsy samples. TBB specimens from patient 3 showed condensed fibromyxoid plugging of alveoli, while autopsy samples show interstitial fibrosis. **F**, Results from severe acute respiratory syndrome coronavirus 2 (SARS-CoV-2) testing by reverse transcription polymerase chain reaction. While TBBs were positive in all patients, one of two and two of two lung autopsy samples were positive in patients 1 and 2, respectively. All autopsy samples were SARS-CoV-2 negative in patient 3.

accumulation of fibrin without hyaline membrane formation FIGURE 1E. Autopsy samples from the same patient showed focal capillary congestion together with microthrombosis and very few fibromyxoid plugs in the alveolar lumen. TBB specimens from patient 2—who was already mechanically ventilated at the time of biopsy—showed alveolar collapse with entrapment of fibrin as well as reactive changes in few pneumocytes. Autopsy samples from the same patient showed widespread fibromyxoid plugging with entrapment of ball-like fibrin and only very few residual ventilated alveoli. In some alveoli, there was a shedding of reactive pneumocytes. In patient 3, TBB specimens showed extensive OP with only very sparse interstitial inflammation. There was extensive cystic change in autopsy samples from the lung periphery in patient 3 together with marked interstitial fibrosis.

SARS-CoV-2 Testing on Tissue Samples and SARS-CoV-2/Angiotensin Converting Enzyme 2/ Transmembrane Protease Serine Subtype 2–FISH

RT-PCR analyses from tissue samples detected SARS-CoV-2 in TBB specimens from all three patients and in both autopsy samples from patient 2 FIGURE 1F. SARS-CoV-2 testing from autopsy samples revealed positivity in one of two samples in patient 1, while both autopsy samples were negative in patient 3. In line with that, SARS-CoV-2 could be detected by FISH in TBB specimens but not in autopsy samples from patients 1 and 3 FIGURE 2. The virus was detected in airway epithelial cells but not in pneumocytes in patient 1. SARS-CoV-2 was detected in both TBB specimens and autopsy samples from patient 2 FIGURE 2. There was only a weak and focal signal for angiotensin converting enzyme 2 (ACE2) in all investigated samples FIGURE 2, while the signal for transmembrane protease serine subtype 2 (TMPRSS2) was strongly detectable in all TBB specimens and autopsy samples from patient 2, correlating with the presence of SARS-CoV-2 FIGURE 2.

Ultrastructural Findings in Lung Autopsy Samples

Electron microscopy (EM) was performed on autopsy samples from all three patients. There was capillary congestion with erythrocytes and fragmentocytes in patient 1. Of note, we observed long and thin cytoplasmic protrusions of erythrocytes consistent with

HTTPS://DOI.ORG/10.1093/AJCP/AQAB087

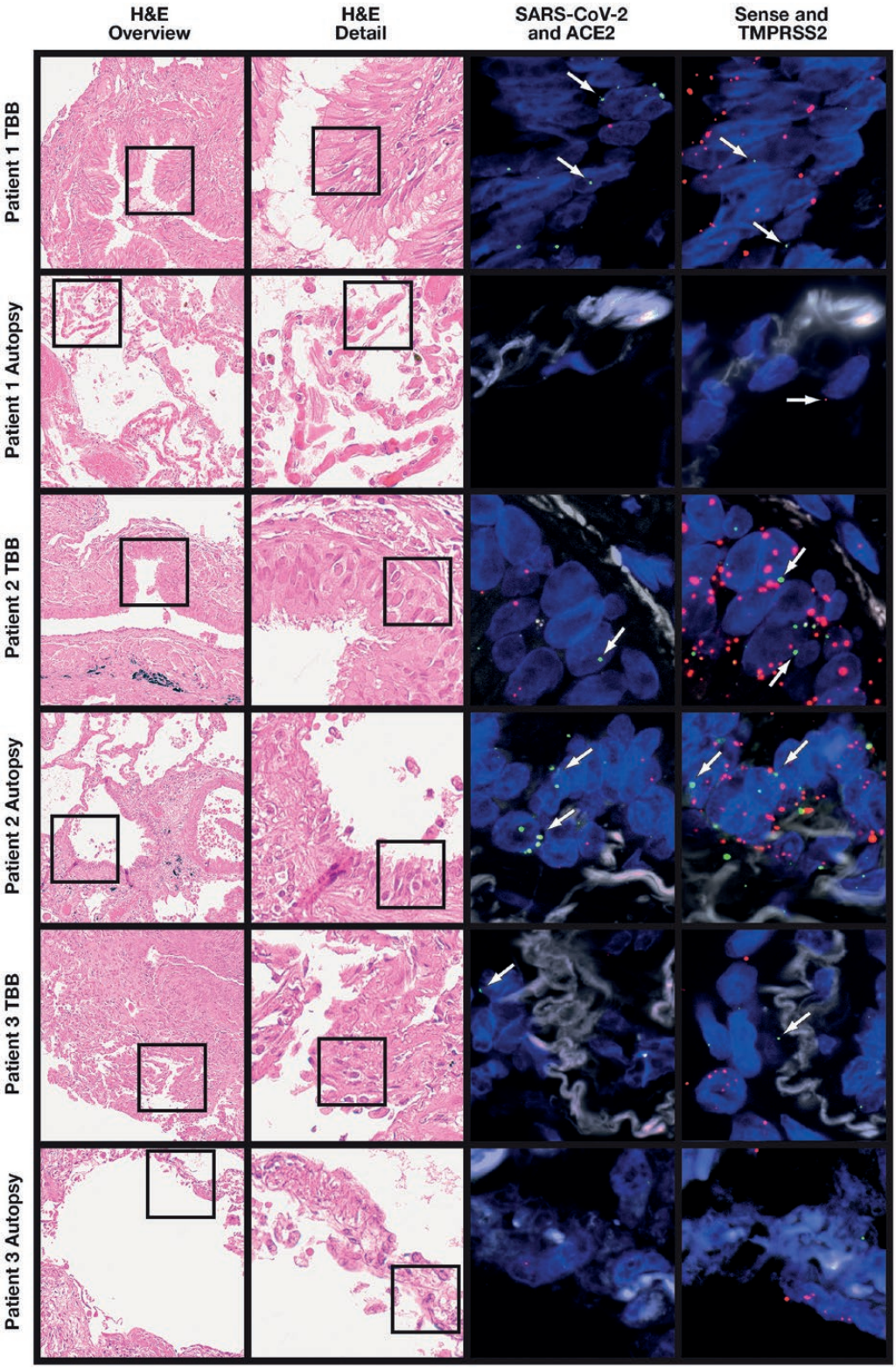

FIGURE 2 Fluorescence in situ hybridization (FISH) of severe acute respiratory syndrome coronavirus 2 (SARS-CoV-2). H&E staining and two combinations of FISH that target SARS-CoV-2 S gene (green) and angiotensin-converting enzyme 2 (ACE2) (red) and replicative SARS-CoV-2–S gene sense (green) and transmembrane protease serine 2 (TMPRSS2) (red) have been performed on consecutive slides. SARS-CoV-2 is strongly expressed in the respiratory epithelium, as shown in the biopsy specimen of patients 1 (arrows) and 2 (arrows) and the autopsy of patient 2 (arrows). To a lower extent, virus could be detected in alveolar epithelial cells, as shown in the biopsy specimen of patient 3 (arrow). High viral replication is detectable in patient 2, as visualized with the V-nCoV2019-S sense probe (green). The receptor TMPRSS2 is strongly expressed, mainly in the respiratory epithelium, similar to the virus (green), whereas ACE2 is only weakly expressed.

HTTPS://DOI.ORG/10.1093/AJCP/AQAB087

acanthocytosis. There was only minimal collagen deposition in the interstitium FIGURE 3A and FIGURE 3B. In patient 2, we observed widespread desquamation of alveolar epithelium, interstitial edema, and deposition of loosely organized collagen in the interstitium FIGURE 3C. There was extensive extracellular matrix deposition containing collagen and elastic fibrils in patient 3 FIGURE 3D. Moreover, we found luminal extension of endothelial protrusions consistent with intussusceptive (splitting) angiogenesis FIGURE 3E.

DISCUSSION

In the current article, we report on antemortem and postmortem pathology in three patients with confirmed SARS-CoV-2 infection, including severe courses of COVID-19. From a clinical viewpoint, all three patients shared established risk factors for a severe disease course (middle or advanced age, cardiovascular risk factors/disease, and/or history of smoking).[19] Laboratory findings at the point of ICU admission showed elevated levels for LDH, D-dimers, IL-6, and CRP, in line with published data.[20] Of note, two of the three patients (patients 2 and 3) tested positive for autoantibodies following previously published guidelines[21] (patient 2: ANA titer 1:1,000; patient 3: positive Scl-70 immunoblot). Previously, it has been shown that detection of autoantibodies is associated with a need for ICU treatment and the occurrence of severe complications in COVID-19.[10] Since all patients were treated in the spring of 2020, no immunosuppressive agents (dexamethasone) had been administered.

Histopathologic findings in lung biopsy specimens from living patients with COVID-19, especially from transbronchial biopsy specimens, have rarely been reported. A very early report described edema, proteinaceous exudate, focal reactive hyperplasia of pneumocytes with patchy inflammation, and multinucleated giant cells in two patients who underwent lobectomy for lung cancer and who were retrospectively found to have COVID-19 at the time of operation.[3] We observed similar changes in patient 1, who was also not yet known to have COVID-19 at the time of biopsy, indicating that pneumocyte hyperplasia with proteinaceous exudate represents the earliest response to SARS-CoV-2 infection. The virus was detected by RT-PCR and FISH, while the latter method demonstrated SARS-CoV-2 in bronchiolar epithelium, where it was coexpressed with TMPRSS2 but not ACE2. This is in line with data from the literature showing that TMPRSS2-expressing cells are highly susceptible to SARS-CoV-2 infection and TMPRSS2 expression might correlate with age, sex, and smoking habits.[22,23] We observed low ACE2 expression in airway epithelial cells in patient 1, consistent with previous reports.[24] Only one of two autopsy samples from patient 1 tested positive for SARS-CoV-2 in RT-PCR, and characteristic histopathologic changes were very focal, supporting the assumption that the patient died early during the disease before widespread involvement of the lung. Such intrapulmonary heterogeneity of SARS-CoV-2 infection has been described, which is why possible sampling errors always have to be considered when interpreting histopathology of COVID-19 lungs.[25] Since the cause of death was pulmonary thromboembolism with high D-dimer levels (>30 mg/L; reference: ≤0.5 mg/L), it is very interesting that electron microscopy showed capillary congestion with erythrocytes and fragmentocytes in this patient. This would be consistent with pulmonary microangiopathy and formation of fibrinous microthrombi in lung capillaries, which seem to be more prevalent in COVID-19 than in influenza-infected lungs.[26,27] Endothelial inflammation and activation of coagulation are associated with multiorgan failure and increased mortality, and antithrombotic drugs have been proposed as potential therapies to prevent thrombosis in COVID-19.[28] Given these findings, we think that patient 1 might represent a mostly vascular pattern of COVID-19–associated lung injury, which has been shown to occur early in the course of the disease,[5] and that these patients might profit from anticoagulative therapy at an early time point. It has to be noted, however, that we did not detect SARS-CoV-2 in endothelial cells in any of the investigated samples, in line with previous reports.[29]

While patient 1 represents an early phase of the host response to SARS-CoV-2 infection, autopsy samples from patient 2 showed widespread DAD with ball-like fibrin and fibromyxoid plugging, consistent with AFOP. This pattern has previously been reported in response to SARS-CoV-2 infection and is believed to represent an intermediate form of lung injury that can be observed in both DAD and OP.[6,7] In line with that, we think that the pattern of lung injury we observed in this patient represents the climax of lung injury in response to SARS-CoV-2 infection, and accordingly, the virus could be detected in all samples from this patient by RT-PCR and FISH. TMPRSS2, but not ACE2, was highly expressed in both respiratory epithelium and pneumocytes in TBB specimens and autopsy samples. Transbronchial biopsy specimens from the same patients taken shortly before death showed alveolar collapse and fibrinous exudate, consistent with an earlier (exudative) phase of DAD.[6] Since it is unlikely that the transition from the exudative to the organizing phase of DAD occurred within less than 48 hours, we think that this finding again reflects the temporal and spatial heterogeneity of histopathologic changes in COVID-19 lungs.[25] Ultrastructural analyses revealed the deposition of collagen fibrils in the interstitium, which might predict interstitial fibrosis but is also a frequent finding in the organizing/proliferative phase of DAD.[30] While we know now that the application of corticosteroids would be beneficial for patients with SARS-CoV-2–induced organizing lung damage, it is unclear whether such treatment would also prevent the development of fibrosis. In patient 3, TBB specimens on day 23 showed extensive organizing pneumonia and only sparse inflammation, while autopsy samples after the patient's death on day 42 showed extensive interstitial fibrosis and peripheral cystic change. The virus was still detectable in TBB specimens, but no virus could be detected by RT-PCR and FISH in autopsy samples. Ultrastructural analyses confirmed extensive collagen deposition. These findings support previous reports describing long-term follow-up of severe COVID-19 and underline the potential of the development of interstitial fibrosis,[31] but it is unclear whether this effect is due to profibrotic properties of SARS-CoV-2 (or the immune response against the virus) or a consequence of lung injury, medication, and/or mechanical ventilation in severe

HTTPS://DOI.ORG/10.1093/AJCP/AQAB087

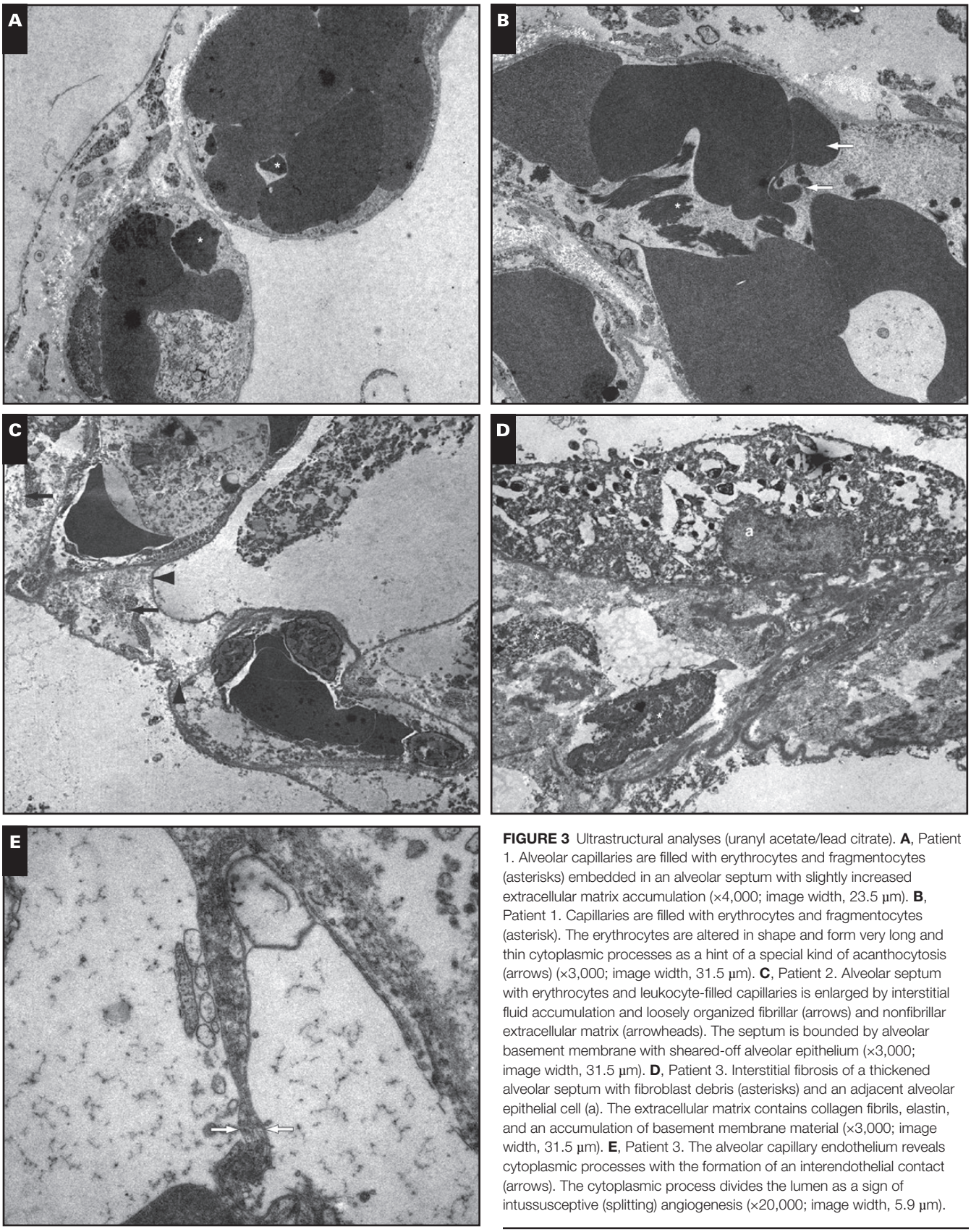

FIGURE 3 Ultrastructural analyses (uranyl acetate/lead citrate). **A**, Patient 1. Alveolar capillaries are filled with erythrocytes and fragmentocytes (asterisks) embedded in an alveolar septum with slightly increased extracellular matrix accumulation (×4,000; image width, 23.5 μm). **B**, Patient 1. Capillaries are filled with erythrocytes and fragmentocytes (asterisk). The erythrocytes are altered in shape and form very long and thin cytoplasmic processes as a hint of a special kind of acanthocytosis (arrows) (×3,000; image width, 31.5 μm). **C**, Patient 2. Alveolar septum with erythrocytes and leukocyte-filled capillaries is enlarged by interstitial fluid accumulation and loosely organized fibrillar (arrows) and nonfibrillar extracellular matrix (arrowheads). The septum is bounded by alveolar basement membrane with sheared-off alveolar epithelium (×3,000; image width, 31.5 μm). **D**, Patient 3. Interstitial fibrosis of a thickened alveolar septum with fibroblast debris (asterisks) and an adjacent alveolar epithelial cell (a). The extracellular matrix contains collagen fibrils, elastin, and an accumulation of basement membrane material (×3,000; image width, 31.5 μm). **E**, Patient 3. The alveolar capillary endothelium reveals cytoplasmic processes with the formation of an interendothelial contact (arrows). The cytoplasmic process divides the lumen as a sign of intussusceptive (splitting) angiogenesis (×20,000; image width, 5.9 μm).

HTTPS://DOI.ORG/10.1093/AJCP/AQAB087

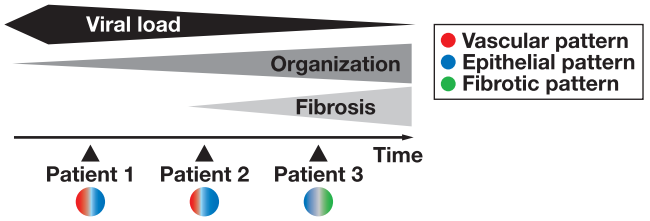

FIGURE 4 Schematic model for the course of coronavirus disease 2019 (COVID-19) and possible implications for long-term sequelae in the lung. While severe acute respiratory syndrome coronavirus 2 viral load increases first and decreases over time, exudative and organizing diffuse alveolar damage exerts deleterious effects on lung function and implies the risk for development of progressive interstitial fibrosis. The different stages in disease progression and the proposed patterns of COVID-19–associated lung injury are reflected by the observed changes in patients 1 to 3.

COVID-19. The finding of a profibrotic autoimmune response (five of six specific autoantibodies associated with sclerosing connective tissue disease) in a previous study would support the idea of COVID-19 directly contributing to fibrotic change in the lung.[10] EM further confirmed the presence of intravascular endothelial protrusions consistent with intussusceptive (splitting) angiogenesis as reported before in ultrastructural analyses of corrosion casts from COVID-19 lungs.[27] In that study, intussusceptive angiogenesis was more frequent in COVID-19 lungs compared with normal lung or lungs from patients with influenza.

Taken together, we show here antemortem and postmortem biopsy specimens from three patients with severe COVID-19, illustrating different patterns of SARS-CoV-2–induced lung injury and histopathologic changes during the disease **FIGURE 4**. Early changes include pneumocyte hyperplasia and capillary congestion, which may be a sign of the risk of thromboembolic complications, especially when high D-dimers are present. At this point, the virus has not necessarily spread throughout the lung. The climax of lung injury is widespread DAD with or without organization, possibly including intermediate AFOP-like patterns; at this point, virus is present in the airways and the lung. When this phase is survived, there is a risk for the development of interstitial fibrosis, but viral load decreases over time and SARS-CoV-2 may not be detected in late-stage disease. The small number of patients and the possibility of sampling errors due to the heterogeneity of pathologic changes in COVID-19 lungs have to be stated as clear limitations to the present study.

Acknowledgments: We thank all patients and their families for their consent to the use of data and images in the present study; Carsten Hackenbroch, MD, for providing imaging data; and the team of the ICU at the Bundeswehrkrankenhaus Ulm for the outstanding quality of care provided to patients with COVID-19.

Disclosure: Drs Gagiannis and Steinestel were speakers for Boehringer-Ingelheim.

REFERENCES

1. Cevik M, Kuppalli K, Kindrachuk J, et al. Virology, transmission, and pathogenesis of SARS-CoV-2. *BMJ*. 2020;371:m3862.
2. Xu Z, Shi L, Wang Y, et al. Pathological findings of COVID-19 associated with acute respiratory distress syndrome. *Lancet Respir Med*. 2020;8:420-422.
3. Tian S, Hu W, Niu L, et al. Pulmonary pathology of early-phase 2019 novel coronavirus (COVID-19) pneumonia in two patients with lung cancer. *J Thorac Oncol*. 2020;15:700-704.
4. Borczuk AC, Salvatore SP, Seshan SV, et al. COVID-19 pulmonary pathology: a multi-institutional autopsy cohort from Italy and New York City. *Mod Pathol*. 2020;33:2156-2168.
5. Polak SB, Van Gool IC, Cohen D, et al. A systematic review of pathological findings in COVID-19: a pathophysiological timeline and possible mechanisms of disease progression. *Mod Pathol*. 2020;33:2128-2138.
6. Nicholson AG, Osborn M, Devaraj A, et al. COVID-19 related lung pathology: old patterns in new clothing? *Histopathology*. 2020;77:169-172.
7. Travis WD, Costabel U, Hansell DM, et al; ATS/ERS Committee on Idiopathic Interstitial Pneumonias. An official American Thoracic Society/European Respiratory Society statement: update of the international multidisciplinary classification of the idiopathic interstitial pneumonias. *Am J Respir Crit Care Med*. 2013;188:733-748.
8. Moore JB, June CH. Cytokine release syndrome in severe COVID-19. *Science*. 2020;368:473-474.
9. Mudd PA, Crawford JC, Turner JS, et al. Distinct inflammatory profiles distinguish COVID-19 from influenza with limited contributions from cytokine storm. *Sci Adv*. 2020;6:eabe3024.
10. Gagiannis D, Steinestel J, Hackenbroch C, et al. Clinical, serological, and histopathological similarities between severe COVID-19 and acute exacerbation of connective tissue disease–associated interstitial lung disease (CTD-ILD). *Front Immunol*. 2020;11:2600.
11. Vlachoyiannopoulos PG, Magira E, Alexopoulos H, et al. Autoantibodies related to systemic autoimmune rheumatic diseases in severely ill patients with COVID-19. *Ann Rheum Dis*. 2020;79:1661-1663.
12. Pascolini S, Vannini A, Deleonardi G, et al. COVID-19 and immunological dysregulation: can autoantibodies be useful? *Clin Transl Sci*. 2021;14:502-508.
13. Woodruff MC, Ramonell RP, Nguyen DC, et al. Extrafollicular B cell responses correlate with neutralizing antibodies and morbidity in COVID-19. *Nat Immunol*. 2020;21:1506-1516.
14. Ferguson ND, Fan E, Camporota L, et al. The Berlin definition of ARDS: an expanded rationale, justification, and supplementary material. *Intensive Care Med*. 2012;38:1573-1582.
15. Murray JF, Matthay MA, Luce JM, et al. An expanded definition of the adult respiratory distress syndrome. *Am Rev Respir Dis*. 1988;138:720-723.
16. Antoch G, Urbach H, Mentzel H-J, et al. SARS-CoV-2/COVID-19: Empfehlungen für die Radiologische Versorgung–Eine Stellungnahme, der Deutschen Röntgengesellschaft (DRG), der Deutschen Gesellschaft für Neuroradiologie (DGNR), der Gesellschaft für Pädiatrische Radiologie (GPR), der Deutschen Gesellschaft für Interventionelle Radiologie (DeGIR), des Berufsverbands der Neuroradiologen (BDNR), und des Berufsverbands der Radiologen (BDR). *Rofo*. 2020;192:418-421.
17. Simpson S, Kay FU, Abbara S, et al. Radiological Society of North America expert consensus statement on reporting chest CT findings related to COVID-19. Endorsed by the Society of Thoracic Radiology, the American College of Radiology, and RSNA–secondary publication. *J Thorac Imaging*. 2020;35:219-227.
18. Hanley B, Lucas SB, Youd E, et al. Autopsy in suspected COVID-19 cases. *J Clin Pathol*. 2020;73:239-242.
19. Wu Z, McGoogan JM. Characteristics of and important lessons from the coronavirus disease 2019 (COVID-19) outbreak in China: summary of a report of 72 314 cases from the Chinese Center for Disease Control and Prevention. *JAMA*. 2020;323:1239-1242.
20. Zhang Z-L, Hou Y-L, Li D-T, et al. Laboratory findings of COVID-19: a systematic review and meta-analysis [published online May 23, 2020]. *Scand J Clin Lab Invest*.

HTTPS://DOI.ORG/10.1093/AJCP/AQAB087

21. Agmon-Levin N, Damoiseaux J, Kallenberg C, et al. International recommendations for the assessment of autoantibodies to cellular antigens referred to as anti-nuclear antibodies. *Ann Rheum Dis.* 2014;73:17-23.
22. Matsuyama S, Nao N, Shirato K, et al. Enhanced isolation of SARS-CoV-2 by TMPRSS2-expressing cells. *Proc Natl Acad Sci U S A.* 2020;117:7001-7003.
23. Piva F, Sabanovic B, Cecati M, et al. Expression and co-expression analyses of TMPRSS2, a key element in COVID-19. *Eur J Clin Microbiol Infect Dis.* 2021;40:451-455.
24. Zhao Y, Zhao Z, Wang Y, et al. Single-cell RNA expression profiling of ACE2, the receptor of SARS-CoV-2. ***Am J Respir Crit Care Med.*** 2020;202:756-759.
25. Desai N, Neyaz A, Szabolcs A, et al. Temporal and spatial heterogeneity of host response to SARS-CoV-2 pulmonary infection. *Nat Commun.* 2020;11:6319.
26. Beigee FS, Toutkaboni MP, Khalili N, et al. Diffuse alveolar damage and thrombotic microangiopathy are the main histopathological findings in lung tissue biopsy samples of COVID-19 patients. *Pathol Res Pract.* 2020;216:153228.
27. Ackermann M, Verleden SE, Kuehnel M, et al. Pulmonary vascular endothelialitis, thrombosis, and angiogenesis in Covid-19. *N Engl J Med.* 2020;383:120-128.
28. McFadyen JD, Stevens H, Peter K. The emerging threat of (micro) thrombosis in COVID-19 and its therapeutic implications. *Circ Res.* 2020;127:571-587.
29. Schaefer IM, Padera RF, Solomon IH, et al. In situ detection of SARS-CoV-2 in lungs and airways of patients with COVID-19. *Mod Pathol.* 2020;33:2104-2114.
30. Fukuda Y, Ishizaki M, Masuda Y, et al. The role of intraalveolar fibrosis in the process of pulmonary structural remodeling in patients with diffuse alveolar damage. *Am J Pathol.* 1987;126:171-182.
31. Aesif SW, Bribriesco AC, Yadav R, et al. Pulmonary pathology of COVID-19 following 8 weeks to 4 months of severe disease: a report of three cases, including one with bilateral lung transplantation. *Am J Clin Pathol.* 2021;155:506-514.

HTTPS://DOI.ORG/10.1093/AJCP/AQAB087